Frequency Offset Estimation of X-band Marine Radar Sampling Signal Based on Phase Difference

Jianming Wang(✉)

Maritime College, Tianjin University of Technology, Tianjin 300384, China
wangjianming@email.tjut.edu.cn

Abstract. Due to the relative radial movement between the transmitter and receiver of marine radar, the frequency of radar sampling signal is prone to deviation, which reduces the quality of radar sampling signal. In order to ensure the effective transmission of radar signals, a frequency offset estimation method of marine radar sampling signals in X-band based on phase difference is proposed. The AD9225 chip is selected to acquire the marine radar signal, and the undersampling theorem is used to determine the marine radar signal sampling frequency, so as to prevent the radar signal from mixing. After digital down conversion processing, two baseband signals are obtained, and the phase information of the radar sampling signal is extracted. Based on the Midamble code, the frequency offset estimation program of marine radar sampling signal is designed. The frequency offset estimation result of the signal can be obtained by executing the established procedure, and the frequency offset estimation of the sampling signal of the X-band marine radar can be realized. Experimental data show that after the application of the proposed method, the minimum signal to noise ratio of radar sampling signal is 4 dB, the minimum mean square error of frequency offset estimation is 4%, and the minimum time of frequency offset estimation is 2 s, which fully confirms that the proposed method has better application performance.

Keywords: X-Band · Sampling Signal · Frequency Offset Estimation · Marine Radar · Phase Difference · Radar Signal Processing

1 Introduction

Navigation radar is an indispensable navigation instrument [1] on the bridge of a ship, which plays a vital role in navigation. Marine radar is a device that uses electromagnetic wave technology to detect targets, so it is not affected by the weather environment, and can detect small and weak targets in a long distance. Navigation radar can accurately detect the distance and direction of target objects, and can achieve target tracking, predict the location and time of encounter with the ship, so as to guide the ship navigation and avoid collision. In the process of marine radar communication, the relative radial movement between the transmitter and receiver will change the frequency of the received

L. Yun et al. (Eds.): ADHIP 2023, LNICST 548, pp. 83–99, 2024.
https://doi.org/10.1007/978-3-031-50546-1_6

signal. This phenomenon is called Doppler effect, and the change of this frequency is called Doppler frequency shift. In addition, the accuracy of the local oscillator and the receiver oscillator will also cause a deviation in the frequency of the received signal, which is called frequency offset, thus affecting the effective transmission of data [2]. However, many factors such as temperature changes, equipment aging, and electromagnetic interference in practical applications may affect the sampling signal of marine radar, resulting in frequency deviation. The frequency offset issue may have a negative impact on the performance of marine radar. For example, frequency offset may lead to errors in distance measurement, inaccurate speed measurement of ships, and even inaccurate target positioning. Therefore, it is very important to accurately estimate and compensate for the frequency offset of marine radar sampling signals.

At present, many scholars have done a lot of research on the estimation algorithm of frequency offset, and also have a lot of research results and a large number of algorithms that can be implemented in practice, and these practical and feasible algorithms and research results will provide important reference and guarantee for improving the performance of frequency offset estimation in the future. Among the frequency offset estimation methods, there are mainly two common methods. The first is the frequency offset estimation method based on the least squares principle. This method is mainly aimed at the frequency offset estimation problem under the medium and high SNR channel conditions. Based on the transformation of additive complex Gaussian noise, the frequency offset estimation process is completed based on the least squares principle [3]. However, this algorithm requires that the phase used for frequency offset estimation cannot change during the whole estimation process; The second is the frequency offset estimation method based on differential phase [4], which uses continuous data frames to reduce the mean square error of the frequency offset estimation value to the GCRLB bound, which is a lower bound than the CRLB of traditional estimation algorithms. Although the above two methods have their own advantages, they also have certain defects, which cannot meet the requirements of marine radar sampling signal frequency offset estimation and restrict the development and application of marine radar. In addition, there is also a blind and simple estimation technique for carrier frequency offset (CFO) of a universal filtered multi carrier (UFMC) system under specified carrier allocation proposed in reference [5]. Reference [6] proposes carrier frequency offset estimation and compensation for MBOFDM ultra wideband systems based on ICA. The Doppler frequency offset estimation for 5G-NR downlink based on deep learning proposed in reference [7]. The autocorrelation method proposed in reference [8, 9], the Maximum likelihood estimation method proposed in reference [10–12], and the Fourier transform method proposed in reference [13–16]. Therefore, a method of marine radar sampling signal frequency offset estimation based on phase difference is proposed. On the basis of obtaining the navigation radar signal, select an appropriate sampling frequency, extract the phase information of the sampled signal, and then perform frequency offset estimation by comparing the phase difference between the reference signal and the sampled signal. By accurately estimating the frequency offset of marine radar sampling signals through phase difference calculation, the performance and accuracy of the radar system can be improved.

2 Frequency Offset Estimation of Marine Radar Sampling Signal

2.1 Marine Radar Signal Acquisition

According to the characteristics of marine radar signal, AD9225 is selected as the marine radar signal acquisition equipment to illustrate the marine radar signal acquisition process. The AD9225 acquisition chip mainly has the following technical performance indicators:

(1) Resolution

AD9225 resolution refers to the fineness of chip scale description, which is usually determined by the number of bits used by AD9225 when outputting digital signals. For example, AD9225 is a 12 bit acquisition chip, and the total voltage range is described by 12 independent binary codes. The absolute voltage unit recognized by the system is lbit [17, 18]. The resolution of AD conversion chip is defined as the ratio of the minimum input analog voltage corresponding to the binary minimum variable to the internal reference voltage of AD, and the expression is

$$2^N = \frac{\alpha}{\beta} \tag{1}$$

In formula (1), N represents the resolution bits of AD9225 chip; α indicates the least significant bit; β indicates the maximum voltage that the AD9225 chip can recognize the analog voltage, and it is also the reference voltage of the AD9225 chip.

(2) Integral Nonlinearity

The integral nonlinearity is defined as the relative deviation between the ideal input conversion level and the actual input conversion level, representing the maximum error between the values collected by AD9225 chip at all sampling points and the true values, in LSB. In order to ensure that AD9225 does not lose code, it is generally specified that the maximum and minimum values of integral nonlinearity are 0.5 LCB and −0.5LSB at 25 °C. The integration nonlinearity is caused by the nonlinearity of ADC's analog front-end, sample holder and ADC's transfer function. The integration nonlinearity is the precision index of AD9225 chip. The smaller the integration nonlinearity, the higher the precision. The calculation formula of integral nonlinearity is

$$\gamma_t = \frac{\hat{Q}_t - \tilde{Q}_t}{\varepsilon_o} \tag{2}$$

In formula (2), γ_t represents the integration nonlinearity of AD9225 chip; $\hat{Q}_t$ and $\tilde{Q}_t$ represents the collected value and the real value at the sampling point of AD9225 chip; ε_o represents the integral nonlinearity calculation error term.

(3) Differential Nonlinearity

Differential nonlinearity is defined as the relative deviation between the actual converted code width and the ideal code width, which is the maximum error of analog quantity between adjacent quantization units of AD9225 chip, and the unit is LSB. In

order to ensure that AD9225 does not lose code [19], it is generally specified that the maximum and minimum values of differential nonlinearity are 0.5 LCB and −0.5 LSB at 25 °C. Due to the deviation of circuit structure and manufacturing process of AD9225 chip itself, the quantization voltage at some points in the range is greater or less than the standard quantization voltage. The resulting error is called differential nonlinearity, and the calculation formula is

$$\gamma_{t-\max} = \frac{\max\left(\hat{Q}_t - \tilde{Q}_t\right)}{\varepsilon_{o-\max}} \tag{3}$$

In formula (3), $\gamma_{t-\max}$ represents differential nonlinearity; $\max\left(\hat{Q}_t - \tilde{Q}_t\right)$ means the maximum value of $\left(\hat{Q}_t - \tilde{Q}_t\right)$; $\varepsilon_{o-\max}$ represents the maximum value of integral nonlinearity calculation error term.

(4) Conversion Rate

The time required for AD9225 chip to convert analog signal to digital signal is called conversion time, and its reciprocal is the conversion rate unit, usually SPS, that is, the number of samples per second. For example, the sampling rate of AD9225 is 25 Msps, that is, the number of samples per second can reach 2.5×10^7. The sampling rate is one of the important technical indicators of the ultra-high speed AD acquisition chip.

(5) Signal-to-Noise Ratio

The signal-to-noise ratio is the dB number of the ratio of the effective value of the signal level to the effective value of various noises (including quantization noise, thermal noise, self noise, etc.) [20]. The signal-to-noise ratio depends on the quantization bits. The larger the number of bits, the smaller the quantization noise. Due to the noise and distortion of the actual AD9225, the actual resolution of the AD9225 is affected and the bits of the AD9225 are reduced. The signal to noise ratio calculation formula is

$$\zeta = \frac{q_1}{q_2} \times 100\% \tag{4}$$

In formula (4), ζ represents the signal to noise ratio; q_1 indicates the number of effective signals in the collected signal; q_2 indicates the number of noise signals in the collected signal.

(6) Noise Power Ratio

The noise power ratio refers to the power ratio of signal to noise. The signal noise ratio is extended to measure the transmission characteristics of frequency division multiplexing communication systems. The noise power ratio is generally represented by the noise power ratio curve [21]. When the input noise level is very low, the noise in the stopband is mainly quantization noise. When the input noise increases, the noise power ratio also increases linearly. The higher the resolution of the AD9225, the smaller the quantization noise and the higher the noise power ratio.

AD9225 chip is a high-performance analog signal acquisition chip with the acquisition rate of 25 MSPS and the resolution of 12 bits. It has built-in on-chip high performance

reference voltage source and sample and hold amplifier. It adopts a multi-stage differential pipeline architecture with built-in output error correction logic. It can provide 12 bit accuracy at 25 MSPS sampling rate and ensure no code loss in the whole operating temperature range. The timing of AD9225 is shown in Fig. 1.

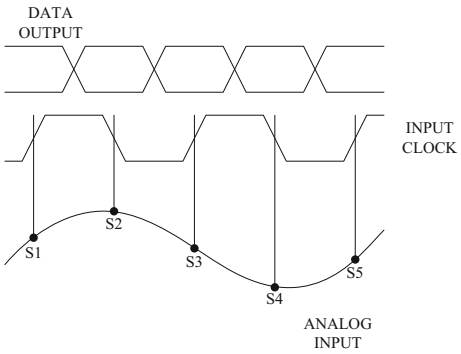

Fig. 1. Timing Diagram of AD9225

As shown in Fig. 1, the sequence diagram is one of the important information to help understand the chip. According to the AD9225 data manual, the sampling data needs to be delayed for 3 clock cycles to complete conversion and output. When the rising edge of the first clock cycle occurs, the sampling and holding circuit inside the AD chip collects the analog voltage at point S1. After voltage comparison and data coding, the analog voltage at point S1 at the rising edge of the fourth clock cycle is converted into a digital signal, and then t_{OD} the data of S1 point sampled at the rising edge of the first clock cycle is DATA1 output [22].

The AD9225 chip selected above is used to collect and acquire marine radar signals, which lays a solid foundation for the subsequent selection of marine radar signal sampling frequency.

2.2 Selection of Marine Radar Signal Sampling Frequency

Since the research target is the marine radar signal in the X-band, the undersampling theorem is used to determine the marine radar signal sampling frequency to prevent the occurrence of radar signal aliasing and facilitate the subsequent frequency offset estimation.

Under sampling theorem [23]: suppose there is a band limited to (f_l, f_h). Analog signal of $x(t)$, its center frequency is f_o, when the sampling frequency meets:

$$f_s = \frac{4f_o}{(2n+1)} \tag{5}$$

In formula (5), f_s represents the sampling frequency; n represents the total number of analog signals, meeting $f_s \geq 2(f_h - f_l)$. It should be noted that $f_o = \frac{f_l + f_h}{2}$.

The sampled radar signal spectrum will periodically extend, and $\frac{f_s}{2}$. The frequency spectrum of the signal at will be symmetrically folded. To avoid overlapping of the lower sidebands, the sampling frequency f_s. It shall meet the following requirements:

$$\frac{2f_h}{n+1} \leq f_s \leq \frac{2f_l}{n} \tag{6}$$

According to the characteristics of the periodic extension of the sampled signal spectrum, select an appropriate filter to filter out the low-frequency components of interest in this paper, thus completing the spectrum shift, that is, the first down conversion. Of course, if the above conditions are met, the premise of no spectrum aliasing after sampling is that the spectrum of the original signal is only limited to a certain frequency band and does not exist in other frequency bands, otherwise, aliasing will occur in the process of spectrum shifting after sampling. For this reason, the actual X-band signal from the radar receiver needs to be passband filtered before A/D sampling to limit the X-band signal to a certain frequency band, and then X-band sampling is carried out according to the above sampling theorem to prevent aliasing.

Based on the above factors and the parameters of the radar receiver studied in this project, according to the conditions that the undersampling theorem should meet, after calculation and comparison, it can be concluded that when $n = 1$ h, sampling rate (f_s) 80 MHz sampling will not cause spectrum aliasing.

The above process completes the determination of marine radar signal sampling frequency, and provides support for the subsequent extraction of marine radar sampling signal phase information.

2.3 Extraction of Phase Information of Marine Radar Sampling Signal

Obtaining marine radar sampling signal under 80 MHz frequency sampling operation $y(t)$, obtained after digital down conversion $I(t)$ and $Q(t)$ for two baseband signals, in order to process clutter and extract targets from radar signals, this paper needs to obtain the characteristic information of radar echoes. Analyzing the amplitude and phase information of the noncoherent radar signal can directly extract more target information from the signal, including the moving speed and target characteristics of the target and other information. In order to obtain the amplitude and phase of the echo signal, it is necessary to extract the envelope and instantaneous phase of the marine radar sampling signal. The envelope and instantaneous phase of the signal can be given by the following formula:

$$\begin{cases} A(t) = \sqrt{I^2(t) + Q^2(t)} \\ \phi(t) = arctg \frac{Q(t)}{I(t)} \end{cases} \tag{7}$$

In formula (7), $A(t)$ represents the envelope of marine radar sampling signal; $\phi(t)$ represents the instantaneous phase of marine radar sampling signal.

The extraction of radar signal amplitude and phase features discussed in this section uses CORDIC (coordinate rotation digital calculation) algorithm, which is implemented in FPGA using CORDIC IP core. Relevant parameters are set through graphical user interface settings (GUI). The functions selected in this paper are Translate function,

structure selection parallel mode, pipeline mode selection maximum mode, output signal selection amplitude and phase output. The calculated value is not truncated, and the input and output are 16 bits, with cache. After the setting is completed, the top-level module - marine radar sampling signal feature extraction module is generated, and its pin definitions are shown in Table 1.

Table 1. Definition of pins of marine radar sampling signal feature extraction module

Pin name	Meaning description
I_in	$I(t)$ Baseband signal input
Q_in	$Q(t)$ Baseband signal input
clk	Baseband signal detection module working clock
phase_out	Calculated phase output, 16 bit signed number output
Z_out	Calculated instantaneous modulus, 16 bit unsigned digital output
rdy	The output data is valid, and the lower module is notified to receive the data

According to the principle of CORDIC algorithm [5, 24], the data input to CORDIC core needs to be converted into data format first. Similarly, the amplitude and phase data output after CORDIC core calculation must also be converted into corresponding data format before entering other subsequent modules for processing.

Through the above process, the phase information of marine radar sampling signal is extracted, which provides a basis for the realization of frequency offset estimation of marine radar sampling signal.

3 Frequency Offset Estimation of Marine Radar Sampling Signal

The phase information of marine radar sampling signal extracted from the above $\phi(t)$ based on the Midamble code, the frequency offset estimation [25] program of marine radar sampling signals is designed. The signal frequency offset estimation results can be obtained by executing the developed program, which provides some help and support for the acquisition and processing of marine radar sampling signals. Since the user data in the data domain of the transmission information will carry the information of frequency offset as the Midamble code sequence, this paper proposes a block frequency offset estimation algorithm based on the Midamble code in the data domain to improve the accuracy of frequency offset estimation. This algorithm iteratively compensates and estimates each sub block of the data field block by block in the same way until the data compensation of the last sub block is completed. Since the frequency offset values generated by adjacent sub blocks are relatively similar, the accuracy of frequency offset estimation can be improved by reducing the estimation error block by block.

Assume that the navigation radar system has achieved ideal timing synchronization, and here the Midamble code of a subframe received by the receiver after passing through

the transmission channel is expressed by formula (8):

$$r_m = \left[\sum_{q=1}^{Q} \left(\chi_{mq}(t) \otimes \delta_{mq}(t) \right) \right] \cdot e^{j2\pi f_D t} + \varepsilon_m(t) \tag{8}$$

In formula (8), r_m represents the Midamble code of a subframe of marine radar sampling signal; $\chi_{mq}(t)$ indicates that the basic Midamble code is rotated in the default way to get the q Midamble code of code track; $\delta_{mq}(t)$ refers to the No q The channel impulse response experienced by the code channel signal, and the window length of the channel impulse response is 16 chips; f_D represents the frequency offset generated by the marine radar sampling signal; $\varepsilon_m(t)$ represents additive complex Gaussian noise [26, 27] with zero mean.

For the signal of a single path, assume that the optimal sampling is achieved in formula (5), that is:

$$g(t) = g_o(t) \otimes g_o(t) = \begin{cases} 0 \ t = \kappa T_C \\ 1 \ t = 0 \end{cases} \tag{9}$$

In formula (9), $g(t)$ represents the best sampling result of marine radar signal; $g_o(t)$ represents the waveform of shaping filter RRC; κ Represents a random integer; T_C represents the signal period of marine radar.

In order to obtain the signal used for frequency offset estimation, it is necessary to $g(t)$ to signal r_m. The impact of will be eliminated $g(t)$ and r_m divide, then you can get;

$$Z_m = \frac{r_m}{g(t)} = e^{j(2\pi f_D T_C + \theta_m)} + \varepsilon_m(t) \tag{10}$$

In formula (10), Z_m represents a signal used for frequency offset estimation; θ_m represents the initial phase of the channel of the Midamble code.

Based on the output result of formula (10), calculate the corresponding average phase difference value. The expression is

$$\Delta\phi_m = \frac{1}{L_m - 1} \sum_{k=0}^{L_m - 2} \arctan\left(\frac{imag(Z_m(k+1)Z_m(k))}{real(Z_m(k+1)Z_m(k))} \right) \tag{11}$$

In formula (11), $\Delta\phi_m$ means average phase difference value of Z_m; $L_m - 1$ means the maximum value of k; $imag(Z_m(k+1)Z_m(k))$ represents the predicted marine radar sampling signal; $real(Z_m(k+1)Z_m(k))$ represents the actual marine radar sampling signal.

According to the calculation result of formula (11), the initial frequency offset estimation result of marine radar sampling signal is

$$f_D = \frac{1}{2\pi T_C} * \Delta\phi_m \tag{12}$$

Data field G Equally divided into m Block, and each sub block is $G_1, G_2, \cdots, G_m$, the estimated value of the initial frequency offset f_D Data compensated to the first sub block

G_1 obtain G_1', because the phase difference between two adjacent symbols in the data domain is $\Delta\phi_{G_1}$ Therefore, the average phase difference between adjacent symbols in the first sub block is f_{D1}. Compensate this frequency offset estimation value to the data of the second sub block G_2 So as to get G_2', and then use the average phase difference method to estimate the frequency offset. Similarly, the average phase difference of the second sub block is $\Delta\phi_{G_2}$, then it can also be obtained that the frequency offset estimation value of the second sub block is f_{D2} [28, 29], and then perform compensation and estimation for each sub block in turn until the m Subblock. G_m is estimated to end when the data compensation of is completed.

Accumulate and average the average phase difference of each sub block mentioned above, and record it as the final frequency offset estimation result of marine radar sampling signal. The expression is

$$\hat{f}_D = \frac{f_{D1} + f_{D2} + \cdots + f_{Dm}}{\tau^o \times \upsilon^a \times m} \tag{13}$$

In formula (13), $\hat{f}_D$ represents the final result of frequency offset estimation of marine radar sampling signal; τ^o and υ^a represents the auxiliary calculation parameter, which determines the accuracy of frequency offset estimation. The value range is [0, 1].

The above process completes the frequency offset estimation of marine radar sampling signals, which provides convenience for the subsequent processing and application of radar signals.

4 Experiment and Result Analysis

The dataset used in the experiment is the MSTAR dataset. MSTAR (Moving and Stationary Target Acquisition and Recognition) is a dataset widely used in radar target detection and recognition research. It contains various types of radar echo data, covering various targets and background conditions. The target types in the dataset include vehicles, buildings, tanks, etc. The MSTAR dataset is commonly used for research on radar target generation, detection, classification, recognition, and other related tasks. Based on this part of the data, the specific preparation and experimental results are shown below.

4.1 Experiment Preparation Stage

The preparation stage is the basis and premise for the smooth experiment. In order to ensure the smooth progress of the experiment, determine the auxiliary calculation parameters τ^o and υ^a. The best value of, set up a variety of experimental conditions, do a good job of experimental preparation. The credibility of the experimental conclusions obtained from a single experimental condition is low. Therefore, 10 experimental conditions are set in this study to maximize the credibility of the experimental conclusions, as shown in Table 2.

As shown in Table 2, the radar sampling signal volume and signal to noise ratio values are inconsistent among the 10 experimental conditions set, indicating that the background environment corresponding to each experimental condition is quite different, which meets the application performance test requirements of the proposed method. It

Table 2. Setting table of test conditions

Test conditions	Radar sampling signal volume/MB	Signal to noise ratio/dB
1	1252	45
2	1024	23
3	985	35
4	1563	30
5	1478	28
6	1952	29
7	1800	32
8	1475	31
9	1632	34
10	1452	37

should be noted that the prepared experimental data has a high signal-to-noise ratio and needs to be processed, which is also the key to verify the application effect of the proposed method.

Auxiliary calculation parameters τ^o and υ^a is closely related to the frequency offset estimation accuracy of the proposed method, so it is necessary to calculate the auxiliary parameters before the experiment τ^o and υ^a determine the best value.

Obtain auxiliary calculation parameters through test τ^o and υ^a. The relationship between and frequency offset estimation accuracy is shown in Fig. 2.

As shown in Fig. 2, when auxiliary calculation parameters τ^o When the value is 0.4, the accuracy of frequency offset estimation reaches 90% of the maximum value. Therefore, determine the auxiliary calculation parameters τ^o the optimal value is 0.4; When auxiliary calculation parameters υ^a. When the value is 0.5, the accuracy of frequency offset estimation reaches the maximum of 96%. Therefore, determine the auxiliary calculation parameters υ^a. The best value is 0.5.

4.2 Analysis of Experimental Results

In order to comprehensively measure the application performance of the frequency offset estimation method of the X-band marine radar sampling signal, the signal to noise ratio of the radar sampling signal, the mean square error of frequency offset estimation and the time of frequency offset estimation are selected as evaluation indicators. Set the frequency offset estimation method based on the least squares principle in reference [3] and the frequency offset estimation method based on differential phase in reference [4] as comparison methods 1 and 2, and design the frequency offset estimation comparison experiment of the X-band marine radar sampling signal. The specific analysis process of the experimental results is as follows:

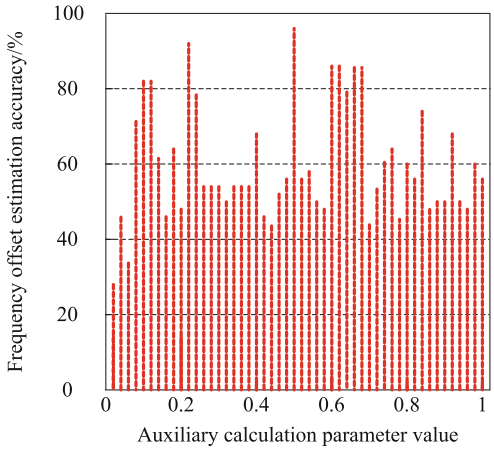

(1) τ^{o} Relation with frequency offset estimation accuracy

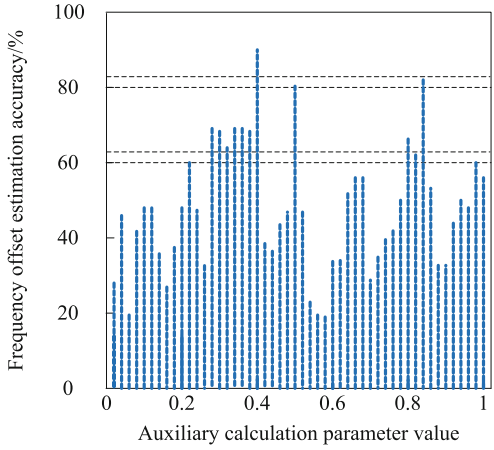

(2) υ^{a} Relation with frequency offset estimation accuracy

Fig. 2. Schematic diagram of the relationship between auxiliary calculation parameters and frequency offset estimation accuracy

4.2.1 Signal to Noise Ratio Analysis of Radar Sampling Signal

The SNR values of radar sampling signals obtained through experiments are shown in Table 3.

As shown in the data in Table 3, after the proposed method, comparison method 1 and comparison method 2 are applied, the signal-to-noise ratio is significantly reduced compared with the prepared experimental data. Among them, the signal-to-noise ratio of the radar sampling signal obtained by the proposed method is generally lower than that of the comparison method 1 and 2, and the minimum value reaches 4 dB, which

Table 3. Signal to noise ratio of radar sampling signal/dB

Test conditions	Propose method	Comparison method 1	Comparison method 2
1	8	15	16
2	6	13	12
3	5	10	10
4	4	11	14
5	10	14	17
6	8	17	19
7	8	10	12
8	7	10	11
9	7	11	12
10	8	14	15

indicates that the proposed method has better denoising effect on the radar sampling signal.

4.2.2 Mean Square Error Analysis of Frequency Offset Estimation

Frequency offset is Frequency modulated wave Frequency swing. Generally speaking, the maximum frequency offset affects the frequency spectrum bandwidth of the FM wave. But it does not mean that the larger the maximum frequency offset is, the wider the spectrum bandwidth will be Modulation index Problems. Generally speaking, the larger the modulation index, the wider the bandwidth of the frequency shift wave spectrum. The maximum frequency offset is a decisive factor of the modulation index, so it affects the spectrum bandwidth of the FM wave. As a phenomenon in frequency modulation, frequency offset is conducive to the transmission of audio information. Under normal frequency offset, the transmission of audio information is guaranteed and is required by audio information in the specified value. The mean square error of frequency offset estimation is easily affected by the X-band frequency. The X-band is mainly divided into the downlink band and the uplink band. The downlink band is 7.25–7.75 GHz, and the uplink band is 7.9–8.4 GHz.

The mean square error of frequency offset estimation in the downlink and uplink bands is obtained through experiments, as shown in Fig. 3.

As shown in the data in Fig. 3, after the proposed method is applied, under the background of downlink and uplink frequency bands, the mean square error of frequency offset estimation obtained is generally lower than that of comparison methods 1 and 2, with the minimum values of 4% and 2% respectively, indicating that the proposed method has better accuracy of frequency offset estimation of radar sampling signals.

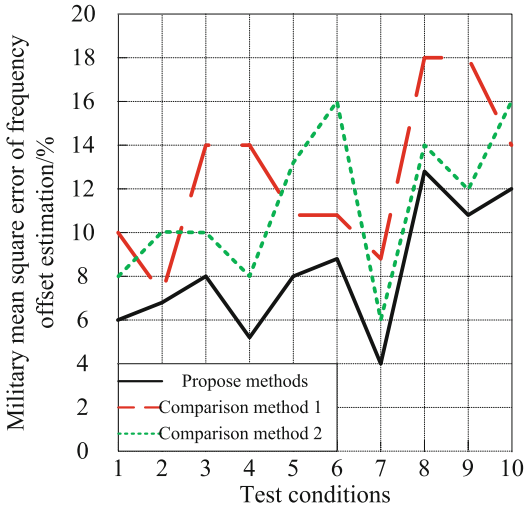

(1) Downlink band

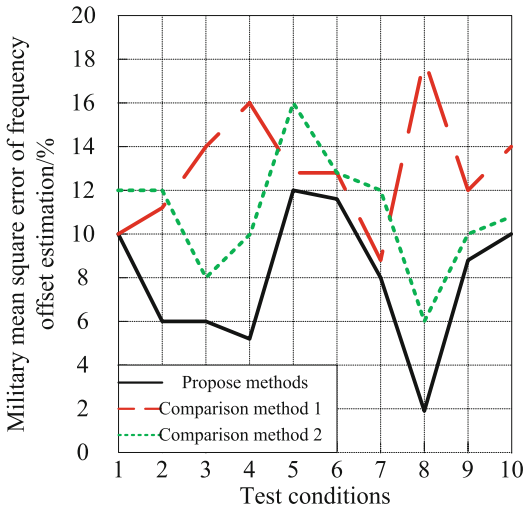

(2) Uplink band

Fig. 3. Schematic diagram of mean square error of frequency offset estimation

4.2.3 Frequency Offset Estimation Time Analysis

Consistent with the mean square error of frequency offset estimation, the frequency offset estimation time will also be affected by the X-band frequency. The X band is divided into the downlink band and the uplink band. The downlink band is 7.25–7.75 GHz, and the uplink band is 7.9–8.4 GHz.

The frequency offset estimation time obtained through experiments is shown in Fig. 4.

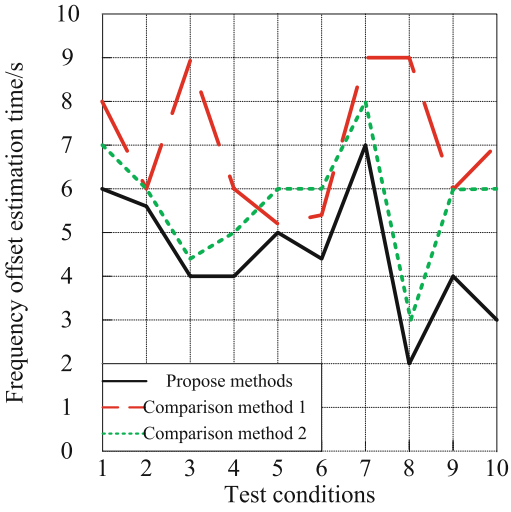

(1) Downlink band

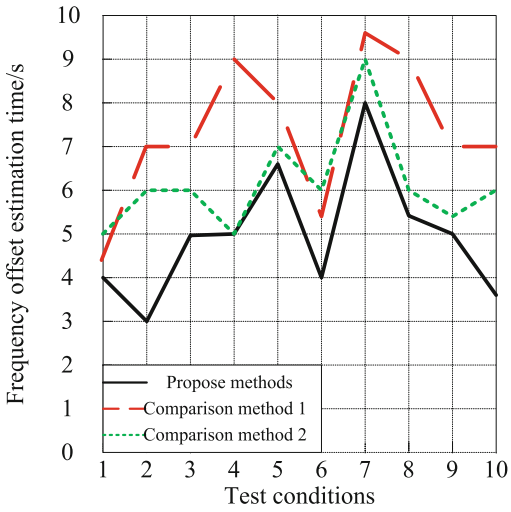

(2) Uplink band

Fig. 4. Schematic diagram of frequency offset estimation time

As shown in the data in Fig. 4, after the proposed method is applied, under the background of downlink and uplink frequency bands, the estimated time of frequency offset obtained is generally lower than that of comparison methods 1 and 2, with the minimum values of 2 s and 3 s respectively, indicating that the proposed method is more efficient in estimating the frequency offset of radar sampling signals.

Set the signal sampling rate to 10 kHz, the signal frequency range to 2 GHz–4 GHz, the frequency offset size to 100 Hz, and the noise level to 20 dB. Introducing a frequency

offset of 100 Hz, three methods were used to test the cumulative phase offset at each sampling point, and the results are shown in Fig. 5.

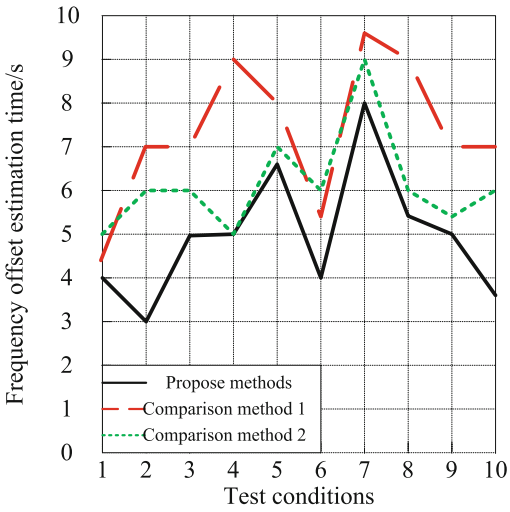

Fig. 5. Schematic diagram of cumulative phase offset

As shown in Fig. 5, the cumulative phase shift of the proposed method is less than 10°, which is lower compared to the two comparison methods. This verifies that the proposed method for estimating the frequency offset of X-band marine radar sampling signals based on phase difference has good estimation performance.

5 Conclusion

With the rise of radar equipment and the expansion of its application range, radar signal processing requirements are getting higher and higher, especially the accuracy of frequency offset estimation. Therefore, the research on frequency offset estimation method of X-band marine radar sampling signal based on phase difference is proposed. The proposed method can reduce the signal to noise ratio of radar sampling signal, reduce the mean square error of frequency offset estimation, and shorten the time of frequency offset estimation, which provides a reference for the frequency offset estimation of marine radar sampling signal.

References

1. Pehlivan, M., Yegin, K.: X-band low-probability intercept marine radar antenna design with improved bandwidth and high isolation. IEEE Trans. Antennas Propag. **69**(12), 8949–8954 (2021)
2. Yang, F., Ma, M.: Data transmission delay compensation algorithm for wireless multi-hop communication network. Comput. Simul. **39**(4), 146–149, 253 (2022)

3. Ali, A., Magarini, M., Pirzada, N., et al.: Direction of arrival and least square error technique used in massive MIMO for channel estimation. Int. J. Math. Comput. Sci. **16**(2), 647–657 (2021)
4. Tajbakhsh, K., Ebrahimi, S., Dashtdar, M.: Low-coherence quantitative differential phase-contrast microscopy using Talbot interferometry. Appl. Opt. **61**(2), 398–402 (2022)
5. Lin, T.T., Hwang, F.H.: Design of a blind estimation technique of carrier frequency offset for a universal-filtered multi-carrier system over Rayleigh fading. IEEE Wirel. Commun. Lett. **11**(5), 1027–1031 (2022)
6. Rajanandhini, C., Babu, S.: ICA based estimation and compensation of carrier frequency offset for MBOFDM based UWB systems. Microprocess. Microsyst. **82**(9), 103824 (2021)
7. Yang, L.H., Zenghao, W., Jie, Z., et al.: Deep learning based Doppler frequency offset estimation for 5G-NR downlink in HSR scenario. High Technol. Lett. **28**(2), 115–121 (2022)
8. Liang, Z., Li, Y., Niu, J., et al.: Fast radar detection method based on two-dimensional trilinear autocorrelation function for maneuvering target with jerk motion. J. Appl. Remote Sens. **15**(2), 026508-1–026508-15 (2021)
9. Ikeda, T., Tsuji, T., Konishi, C., et al.: Spatial autocorrelation method for reliable measurements of two-station dispersion curves in heterogeneous ambient noise wavefields. Geophys. J. Int. **226**(2), 1130–1137 (2021)
10. Peng, J., Rajeevan, H., Kubatko, L., et al.: A fast likelihood approach for estimation of large phylogenies from continuous trait data. Mol. Phylogenet. Evol. **161**(4), 107142 (2021)
11. Candan, Ç., Çelebi, U.: Frequency estimation of a single real-valued sinusoid: an invariant function approach. Sig. Process. **185**, 108098 (2021)
12. Zhang, J.F., Wang, F.Y., Ye, S.U., et al.: Research on power grid primary frequency control ability parallel computing based on multi-source data. Acta Automatica Sinica **48**(6), 1493–1503 (2022)
13. Li, R., Xuan, J., Shi, T.: Frequency estimation based on symmetric discrete Fourier transform. Mech. Syst. Sig. Process. **160**, 107911 (2021)
14. Liang, Y., Zhang, Z., Li, H., et al.: A robust and accurate discrete Fourier transform-based phasor estimation method for frequency domain fault location of power transmission lines. IET Gener. Transm. Distrib. **16**(10), 1990–2002 (2022)
15. Chen, G., et al.: Real-time reception of NHS-OFDM signal with SPA-enhanced channel estimation for intensity-modulated direct-detection systems. Chin. Opt. Lett. **20**(5), 050601 (2022)
16. Chui, C.K., Jiang, Q., Li, L., Jian, Lu.: Analysis of an adaptive short-time Fourier transform-based multicomponent signal separation method derived from linear chirp local approximation. J. Comput. Appl. Math. **396**, 113607 (2021)
17. Tse, J.R., Shen, L., Shen, J., et al.: Nyquist sampling theorem and Bosniak classification, version 2019: effect of thin axial sections on categorization and agreement. Eur. Radiol. **32**(12), 8256–8265 (2022)
18. Qi, B., Zhang, H., Zhang, X.: Time-frequency DOA estimation of chirp signals based on multi-subarray. Digit. Sig. Process. **113**, 103031 (2021)
19. Qi, Hu., Keating, S., Innanen, K.A., Chen, H.: Direct updating of rock-physics properties using elastic full-waveform inversion. Geophysics **86**(3), MR117–MR132 (2021)
20. Changela, A., Zaveri, M., Verma, D.: Mixed-radix, virtually scaling-free CORDIC algorithm based rotator for DSP applications. Integration **78**(May), 70–83 (2021)
21. Kiefer, M., et al.: IMK/IAA MIPAS temperature retrieval version 8: nominal measurements. Atmos. Meas. Techn. **14**(6), 4111–4138 (2021)
22. Hadei, S.A., Abolfazl Hosseini, S., Miri, M.: Performance analysis of the low-complexity adaptive channel estimation algorithms over non-stationary multipath Rayleigh fading channels under carrier frequency offsets. IET Commun. **16**(9), 988–1004 (2022)

23. Wang, D., Zhang, S., Liu, J., Yuan, L., Gao, G.: Modified frequency-domain channel-estimation based on the dual-dependent pilots for polarization-division-multiplexed coherent optical orthogonal frequency division multiplexing systems with offset-quadrature-amplitude modulation. Opt. Eng. **61**(06), 066109-1–066109-14 (2022)
24. Nachaoui, M., Laghrib, A., Afraites, L., et al.: A non-convex non-smooth bi-level parameter learning for impulse and Gaussian noise mixture removing. Commun. Pure Appl. Anal. **21**(4), 1249–1291 (2022)
25. Jeong, S., Farhang, A., Perovic, N.S., Flanagan, M.F.: Low-complexity joint CFO and channel estimation for RIS-aided OFDM systems. IEEE Wirel. Commun. Lett. **11**(1), 203–207 (2022)
26. Wang, C., Zhang, X., Li, J.: FDA-MIMO radar for DOD, DOA, and range estimation: SA-MCFO framework and RDMD algorithm. Sig. Process. **188**, 108209 (2021)
27. Shi, Q., Liu, M., Hang, L.: A novel distribution system state estimator based on robust cubature particle filter used for non-gaussian noise and bad data scenarios. IET Gener. Transm. Distrib. **16**(7), 1385–1399 (2022)
28. Wang, Y.Y., Yang, S.J.: Estimation of carrier frequency offset and channel state information of generalize frequency division multiplexing systems by using a Zadoff-Chu sequence. J. Franklin Inst. **359**(1), 637–652 (2022)
29. Yaşar, C.F.: Algebraic estimator of Parkinson's tremor frequency from biased and noisy sinusoidal signals. Trans. Inst. Measure. Control **43**(3), 679–686 (2021)